^{1}H NMR Characterization of the CdSe Nanocrystallite Surface

Sara A. Majetich,*,† Adriaan C. Carter,† John Belot,‡ and Richard D. McCullough*,‡

Departments of Physics and Chemistry, Carnegie Mellon University, Pittsburgh, Pennsylvania 15213

Received: August 9, 1994⊗

Proton NMR measurements are used to study the kinetics and equilibrium binding of *n*-butanethiolate (BuS^-) to the surfaces of CdSe nanocrystallites and the chemistry induced by CdSe surfaces. Because these crystallites have a well-defined size and shape, the overall amount of attached ligand can be determined by NMR and related to the average number of attached groups per nanocrystallite. Evidence of catalytic generation of *n*-butyl disulfide (BuSSBu) at the nanocrystallite surface is observed by NMR and by GC/MS measurements. The connection between NMR and luminescence measurements is made, and these results are used to model the surface attachment on CdSe nanocrystallites.

Introduction

Cadmium selenide nanocrystallites have been studied extensively by optical techniques,[1−3] yet many questions remain concerning their surfaces. In both physical and electronic structure, nanocrystallites fall between the molecular and bulk solid regimes. These clusters of atoms have no set molecular formula, and even the highest quality nanocrystallite samples have variations both in the number of (CdSe) units and in the number of attached surface ligands. However, some control over both physical structure and number of atoms and ligands can be found in the cadmium selenide nanocrystallites used in the study presented here. CdSe can also be probed optically and structurally, and the photophysical properties can be tuned by varying the amount and type of ligand attached. The electron−hole recombination on a nanosecond time scale and the photoluminescence quantum yield have been shown to depend markedly on the functional groups attached to the CdSe surface.[4] The goal of this work is to establish a method for quantifying the number of groups attached and to demonstrate a correlation between surface passivation and the optical emission properties of semiconductor nanocrystallites.

This work builds on previous results from several groups. Solution proton NMR has been used to study the surface of closely related CdS nanocrystallites capped with thiophenol.[5] This work found that the surface coverage depended inversely on nanocrystallite size, and T_2 data for nanocrystallites below their maximum coverage implied that the attached groups were clustered together on the nanocrystallite surface. An X-ray diffraction study of $Cd_{32}S_{14}(SC_6H_5)_{36}\cdot(DMF)_4$ crystals suggested that tiny nanocrystallites may have cubic cores surrounded by a hexagonal exterior.[6] The crystal structure showed that two different types of Cd−thiolate bonding existed. In a departure from previous models of the CdSe nanocrystallite surface, the crystal structure indicated that the thiophenolate groups were attached in bridging positions along facets of the hexagonal CdSe outer layer. It should be noted that the relationship between the solution structure and bonding of the ligands is at this point only speculative. ^{13}C and ^{113}Cd NMR of smaller cadmium sulfide clusters[7,8] have been used to distinguish bridging and terminal bonding of capping ligands. Studies of the effect of amine surface groups attached to bulk CdSe have shown enhanced photoluminescence, attributed to a reduced depletion width.[9] Similar effects have been noted in CdSe nanocrystallites;[4] however, the mechanism may be different since the depletion width, if it existed, would be larger than the crystallite diameter. Finally, redox reactions and photochemistry at bulk CdS and CdSe surfaces have been studied as a function of the attached ligand.[10] These reactions include light induced catalytic conversion of organic thiols to disulfides, which was expected to be pertinent to our thiolate-functionalized nanocrystallite surfaces.

The ^{1}H NMR results presented here will first be used to determine the average number of ligands attached to the nanocrystallite surface. Next the use of NMR to investigate the kinetics of ligand attachment and detachment at the nanocrystallite surface will be described and compared with photoluminescence results. The catalytic generation of butyl disulfide at the nanocrystallite surface will be demonstrated by a series of NMR experiments in conjunction with GC-MS. Finally, these results will be combined with those of earlier studies to develop a more detailed understanding of the CdSe nanocrystallite surface.

Experimental Section

CdSe Nanocrystallite Preparation. A colloidal solution (1300 mL) containing 35 Å diameter nanocrystallites was prepared using standard inverse micelle techniques explained in more detail elsewhere.[11] The solution contained a mixture of heptane and nanopure water with AOT (bisdioctyl succinate) as a surfactant, and $Cd(ClO_4)_2\cdot 6H_2O$ and $((CH_3)_3Si)_2Se$ were added to generate nanocrystallites within the inverse micelles. The crystallite surfaces were passivated by adding an excess (3−4 mL) of pyridine to this solution, causing instantaneous precipitation.

To remove AOT and other impurities from the nanocrystallites, an improved purification procedure was developed. The crystallite-containing powder was filtered and washed repeatedly with a mixture of pyridine and hexane. Petroleum ether was used in earlier preparations, but this was later found to contain trace amounts of butanethiol, which would complicate our NMR analysis. While the powder was still moist after its first precipitation, it was divided and placed into four 50 mL centrifuge tubes. All of the powder went into solution after 25 mL of pyridine was added to each tube, and the tubes were shaken vigorously. Hexane (25 mL) was then added to precipitate the nanocrystallites again. The tubes were then

* To whom correspondence should be addressed.
† Department of Physics.
‡ Department of Chemistry.

0022-3654/94/2098-13705$04.50/0

sealed and centrifuged at 430 g for 7 min. The supernatant was decanted off, and if it was not colorless, the procedure was repeated using a reduced volume of pyridine and a larger volume of hexanes. The cleanest samples were produced by repeating the precipitation procedure approximately 10 times, as determined by NMR. The samples were then air dried, and clumps were then crushed to a powder, and dried further under vacuum. To ensure that the TEM, X-ray diffraction, and elemental analysis measurements were applicable to the nanocrystals studied in solution, we performed these measurements only on the portion of the powder which was soluble after the washing procedure. Absorption spectra were taken to ensure that the size distributions remained the same. Elemental analysis (Galbraith Laboratories, Knoxville, TN) was done to verify the sample purity and to determine the number of nanocrystallites/mg of sample, in conjuction with TEM measurements, which measured the nanocrystallite size.

NMR Samples. Identification of the proton absorptions was accomplished through a series of high-resolution solution ^1H NMR measurements, beginning with pure samples. These results were found to be reproducible from sample to sample. CdSe nanocrystallites were synthesized immediately prior to use. For the control NMR spectra, 50 μL of the desired compound and 1.00 mL of pyridine (99.5% d_5, Aldrich) were placed in an NMR tube under argon, and the tube was then sealed. The *n*-butanethiol and butyl disulfide reagents were dried over CaH_2, distilled, and stored in a drybox. For control samples used to identify the presence of AOT impurities, 10.0 μmol of AOT was dissolved in 1.00 mL of pyridine-d_5.

NMR spectra of nanocrystallite samples capped with pyridine and *n*-butanethiolate (BuS^-) surface ligands were also studied. For the pyridine-capped nanocrystallites, pyridine-d_5 (1.00 mL) was placed in a clean sample vial, and 60 mg of dried pyridine-capped nanocrystallites was added to the solvent. The vial was sealed and sonicated for 20 min until the powder was dissolved. The suspension was then centrifuged at 430 g for 7 min. The clear, dark orange supernatant was transferred to an NMR tube, leaving behind 20 mg of undissolved solid. The tube was then filled with argon and sealed.

The butanethiolate-capped nanocrystallites were prepared by placing pyridine (50.0 mL) in a 100 mL round-bottom flask, to which 80 mg of pyridine-capped nanocrystallites was added, and the mixture was allowed to stir overnight. After stirring, most of the nanocrystallites dissolved, although some cloudiness persisted. Butanethiol (1.00 mL) was added and the solution was allowed to stir for 2 days in order to eliminate the cloudiness. The nanocrystallites were then washed three times with the centrifuge method described above and dried, and the NMR samples were prepared in the same way as the pyridine-capped nanocrystallites.

Samples used to observe competition in surface binding between butanethiol (BuSH) and pyridine were prepared as follows. A pyridine-capped sample was prepared as described above and butanethiol (3.0 μL) was added immediately before the NMR measurements.

NMR Experiments. ^1H NMR spectra were recorded on an IBM Bruker FT300 NMR spectrometer. All 300 MHz ^1H NMR spectra were done in pyridine (99.5% d_5) and are reported in ppm as δ referenced to residual protons in pyridine-d_5. Spectra were obtained using a delay time of 4 s, which is on the order of T_1 for all the protons in question. The acquisition times used were 2.7 μs, and the pulse width was 9 μs. Where intensities were compared, the spectrometer was run in the absolute intensity mode. Homonuclear coupling experiments were done using standard saturation decoupling with minimum decoupling needed for saturation. Every absorption was decoupled in order to make the NMR assignments. The T_1 experiments were performed using standard inversion–recovery pulse sequences ($\pi-d-\pi/2$).[12] Prior to the T_1 experiments the 90° pulse was determined for H_2 protons (Figure 1a) to be 9.9 μs. The longest delay (d) between pulses was always greater than $5T_1$, affording a reliable source of system reequilibration.

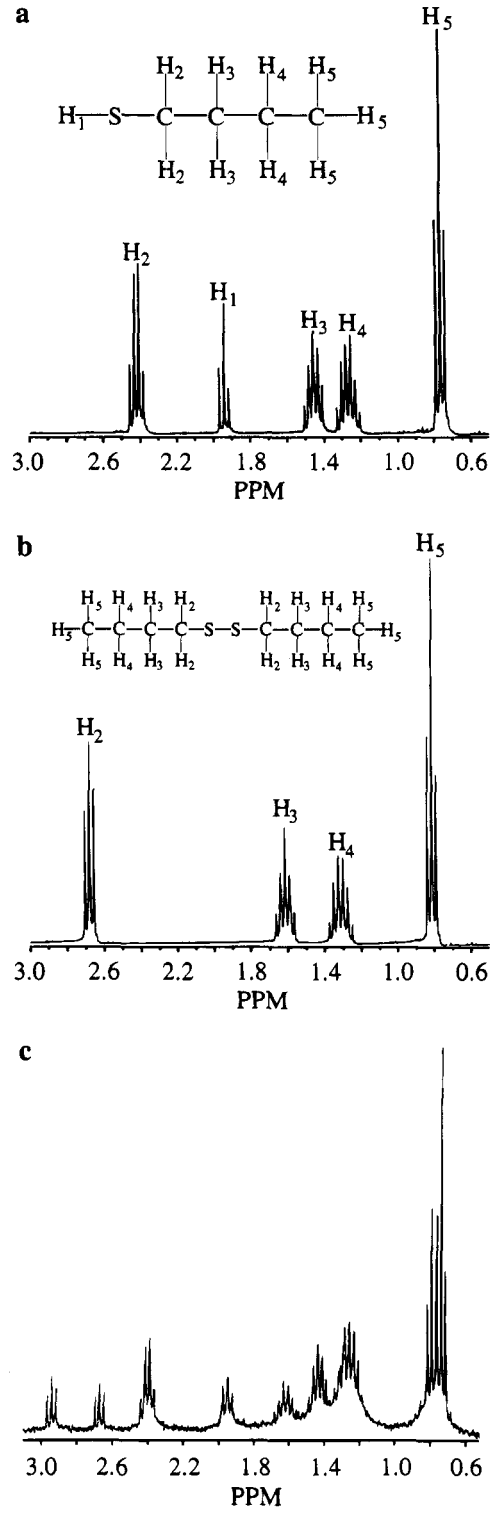

Figure 1. (a) ^1H NMR spectrum of butanethiol in pyridine-d_5, with chemical shifts indicated in PPM. (b) Spectrum for butyl disulfide in pyridine-d_5. (c) Spectrum of a nanocrystallite sample originally capped with pyridine, shortly after the addition of butanethiol. In addition to the free butanethiol resonances indentical to those in (a), new multiplets due to attached ligands are observed.

Gas Chromatography. Gas chromatography/mass spectroscopy was done using a Hewlett-Packard 59980 GC-MS workstation on samples diluted with degassed, dry benzene. The GC column was a Hewlett-Packard fused silica capillary column cross-linked with 5% phenylmethylsilicone.

Luminescence Measurements. Previous studies of surface effects in CdSe nanocrystallite luminescence[4] have shown similar spectral shapes but larger quantum yields for similarly prepared BuS^--capped compared with pyridine-capped crystallites. Here luminescence measurements were performed on samples to monitor the BuS^- attachment to the surface and to compare the results with the kinetics and surface coverage shown by NMR. The same concentrations were used in both the photoluminescence and the NMR experiments.

For room-temperature photoluminescence measurements, a pyridine-capped nanocrystallite solution was first transferred to a quartz cuvette. In these experiments the sample cuvette was excited by 6 ns pulses from a Spectra Physics GCR3 Nd:YAG laser-pumped tunable dye laser. The dye laser wavelength was adjusted to pump the first excited state of the predominant nanocrystallite size (at 510 nm). Emission was monitored at right angles to the laser beam by a C VI Digikrom 480 monochromator with a Hamamatsu R926 photomultiplier tube.

After a spectrum was taken for the pyridine-capped nanocrystallite solution, BuSH was injected while the luminescence at its peak wavelength was detected as a function of time. The same concentration was used as in the NMR experiment, and the solution was stirred. Finally, the equilibrium photoluminescence spectrum was taken.

Results

Peak Identification. Our results show that high-resolution ^1H NMR can distinguish butanethiolate attached to the nanocrystallites from "free" butanethiol in solution. A ^1H NMR spectrum of BuSH in pyridine-d_5 is shown in Figure 1a, along with the assignment of the proton peaks. Both H_1 and H_5 are triplets, but the H_1 peaks are absent in butyl disulfide (Figure 1b). In BuSH H_2 is split by H_1 and H_3 to form a quartet, but in the BuSSBu it is split only by H_3 and forms a triplet. H_3 and H_4 give rise to a quintet and sextet, respectively.

The NMR spectrum of BuS^- group attached to the nanocrystallite surface is expected to look very similar to that of BuSSBu (Figure 1b). In both cases the H_1 proton is missing, and H_2 is a triplet rather than a quartet. Figure 1c shows the ^1H NMR spectrum of a noncrystallite sample just after the addition of BuSH. In addition to the free BuSH peaks identical to those in Figure 1a, several new peaks appear. A triplet centered at 2.94 ppm grows rapidly but starts to disappear after approximately 6 h and is gone after 2 days. Another triplet occurs at 2.67 ppm and is assigned to the H_2 proton in agreement with that for BuSSBu. The H_3 quintet is downshifted to approximately 1.65 ppm. The assignment of the H_4 peak position for attached BuS^- is difficult because of the overlap with the free BuSH H_4 sextet, but in BuSSBu this shift is seen to be small. The H_5 triplet also undergoes a small shift for BuS^--capped nanocrystallites and in BuSSBu.

In each sample containing mixtures of free butanethiol and/or butane disulfide and/or BuS^--capped nanocrystallites, each and every ^1H NMR peak was decoupled in order to unequivocally establish the proton assignments. In addition to ^1H NMR homonuclear decoupling experiments, rigorously purified standard samples of BuSH, BuSSBu, and BuS^--capped nanocrystallites were examined by ^1H NMR and the peaks matched to mixture samples. These experiments were reproduced several times in order to make proton assignments.

Butyl Disulfide Generation. We have found small amounts of butyl disulfide, based on GC-MS measurements of the supernatant after the nanocrystallites were precipitated out of solution with hexane or benzene. Since pyridine-capped nanocrystallites treated directly with BuSSBu and then washed show no evidence of direct attachment, BuSSBu is believed to be generated in situ from neighboring BuS^-groups attached to the surface. Precipitation of the BuS^--capped nanocrystallites followed by extensive washing of the precipitate with benzene removes essentially all the BuSSBu. When samples of purified, O_2-free BuSH in pyridine were examined under identical conditions, no BuSSBu was observed.

Both butanethiolate ligands and butyl disulfide have NMR peaks at 2.67 ppm, and their contributions were differentiated in the following way: After the transient signal at 2.94 ppm disappeared, the nanocrystallites were washed by precipitation with deuterated benzene, centrifugation, and then redispersion in deuterated pyridine. This reduced the signal at 2.67 ppm *after reprecipitating* to 15% of its initial value and was not changed by further washing. After reprecipitating the nanocrystallites, butyl disulfide was no longer observed by GC-MS. Nanocrystallites after precipitation in benzene-d_6 therefore have no contribution from BuSSBu to the NMR signal, either in solution or weakly attached to the surface. Further addition of BuSH causes the transient NMR peak at 2.94 ppm to reappear and the 2.67 ppm peak to grow.

The difference between BuS^- bound to CdSe nanocrystallites and free BuSSBu was also characterized by T_1 measurements of the peak at 2.67 ppm, which represents the H_2 proton shift in Figures 1b,c. As standards, the T_1 of a solution of BuSSBu was determined to be 3.0 ± 0.1 s, and a solution of *n*-butanethiol had a T_1 of 2.5 ± 0.1 s. For the washed nanocrystallite sample, which contains only bound butanethiolate, the T_1 of the 2.67 ppm peak was found to be 4.0 ± 0.1 s. T_1 should be longer for a bound butanethiolate since the degrees of freedom are reduced and the predominant relaxation is suppressed. In addition, the rotational correlation times should be reduced, increasing the relaxation time. Although it has been shown[5] that the correlation times are size dependent in nanocrystallite samples, our average sample size is fixed. In addition the assignment of the 2.67 ppm peak as the bound BuS^- attached to CdSe nanocrystallites is similar to previously reported shifts of the α proton (2.61 ppm) in $Cd(SC_3H_7)_4$ complexes.[8]

Surface Coverage. The relative amounts of attached and unattached BuSH in our samples at equilibrium were determined by integrating the intensity of the H_2 triplet in each. A known amount of methylene chloride was added to each sample as a check on the intensity standard. The H_2 peak was selected because it was not obscurred by overlapping peaks.

To relate this to the average number of ligands per nanocrystallite, the number of nanocrystallites in our sample was determined from the elemental analysis and TEM results. TEM indicated crystalline particles with an average diameter of 35 Å (±10%), and the images showed no evidence of the surface ligands. Assuming this diameter corresponds to the CdSe core, an average nanocrystallite contains 811 atoms, plus the surface ligands.

The elemental analysis data for a carefully washed BuS^--capped nanocrystallite sample were interpreted in the following way.[13] First the Cd and Se atoms were distributed into 811-atom nanocrystallites using the experimentally determined abundances. While the sample was found to be slightly Cd-rich, the Cd:Se ratio is close to one-to-one, as expected. All of the S was assumed to exist as part of a SC_4H_9 group, and the number of BuS^- groups per nanocrystallite was determined to

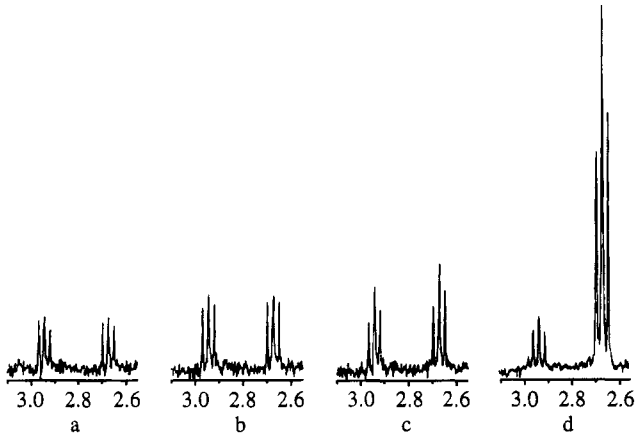

Figure 2. Expanded region of the spectrum described in Figure 1c, showing the peaks centered at 2.67 and 2.94 ppm at various times after the addition of butanethiol: (a) 2 min; (b) 1 h; (c) 6 h; (d) 48 h.

be 26. Finally, N was assumed to exist only as C_5H_5N, and the number of pyridine molecules per nanocrystallite was calculated to be 120. Following these arguments 99.16% of the mass in our sample was accounted for. Using the "molecular weight" found from elemental analysis to calibrate the NMR intensities, we found 22.6 ± 6.5 H_2 proton pairs per nanocrystallite. Here the main source of error is found in the nanocrystallite size distribution.

Models are needed to estimate the number of Cd surface sites available for bonding in order to relate the number of ligands per nanocrystallite to the degree of surface coverage. While elemental analysis does not directly determine the degree of surface coverage, since solvent molecules could be trapped between particles, it yields an upper limit. A spherical shell model[14] has previously been used to estimate the number of atoms in the core of a nanocrystallite with a given radius.[5] It agrees with the experimentally measured Cd:Se abundance ratio and predicts 126 surface Cd sites for a Se-centered nanocrystallite. However, if this model is applied to a Cd-centered nanocrystallite, the number of Cd surface sites is reduced by one-third and the abundance ratio is inconsistent with experiment. A more detailed description of an alternative model is reported elsewhere.[13] This model assumes that the nanocrystallite will remain approximately neutral as it grows, with surface ligands balancing the excess charge of the Cd_xSe_y cluster, without specifying a central atom. We find the surface site estimate to be consistent with that for the Se-centered nanocrystallite.

Kinetics. Unfortunately, the ^1H shifts between pyridine attached to the nanocrystallites and pyridine in solution were too small to differentiate these species; however, we were able to study the kinetics of BuSH displacement of surface pyridine groups by NMR. When a small amount (3 μL) of BuSH was added to the solution of pyridine-capped nanocrystallites in pyridine-d_5, the peaks due to BuS^- attached to the nanocrystallites appeared and grew. Both the H_2 triplet at 2.67 ppm and the transient peak at 2.94 ppm (Figure 1c) appeared immediately, but the transient peak grew more rapidly at first (Figure 2). The rapid initial growth phase occurred in less than 1 min. However, the transient peak disappeared after a few days while the 2.67 ppm triplet grew slowly until the BuSH was used up. Homonuclear decoupling experiments identified both of these peaks as belonging to BuS^- H_2 protons. Therefore we observed two types of BuS^- ligands bound to the nanocrystallite surface.

The luminescence intensity time profile also increased with time, like the H_2 NMR peak intensity (Figure 3a), but the time

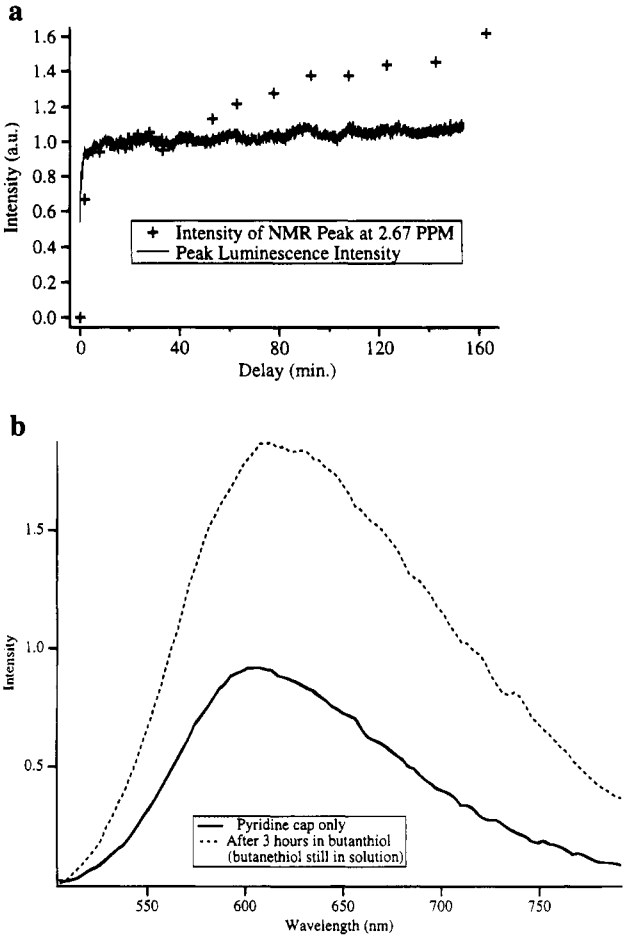

Figure 3. Photoluminescence intensity of a pyridine-capped nanocrystallite solution after the addition of butanethiol. In addition to free butanethiol resonances, new multiplets due to attached ligands are observed. (b) Photoluminescence intensity (au) as a function of wavelength for the initial pyridine-capped nanocrystallite sample, and for the same sample 3 h after the injection of butanethiol.

dependence was somewhat different. The samples used here exhibit trap state luminescence (Figure 3b). Since many trap states are located at the surface, luminescence is sensitive to surface treatment. The lower curve shows the luminescence of pyridine-capped CdSe nanocrystallites before the addition of BuSH. The photoluminescence lifetime as a function of surface treatment was also measured, but no differences were found. The results was actually an upper limit due to the laser pulse duration and the detection electronics. A similar lifetime, coupled with the fact that the emission spectra for different surface treatments differ only in magnitude, suggests that the trap states are involved in the photoluminescence. The change in luminescence intensity correlates well with that of the H_2 NMR peak at early times, while at later times the luminescence intensity levels off while the NMR signal at 2.67 ppm continues to grow. One possible reason for this discrepancy is that the 2.67 ppm resonance includes contributions from both attached BuS^- ligands and from BuSSBu.

We have also observed the generation of BuSSBu after exposure of the nanocrystallite samples to ambient light. We have carefully identified the disulfide peaks by decoupling experiments, spiking NMR samples, and GC-MS analysis as a function of time. It is well-known that CdS and CdSe surfaces catalyze the photochemical oxidation of RSH to RSSR and that quantitative conversion of RSH to RSSR is found after irradiation of CdS at 632 nm.[10] We find that ambient light produces steady but low yields of the disulfide in the nano-

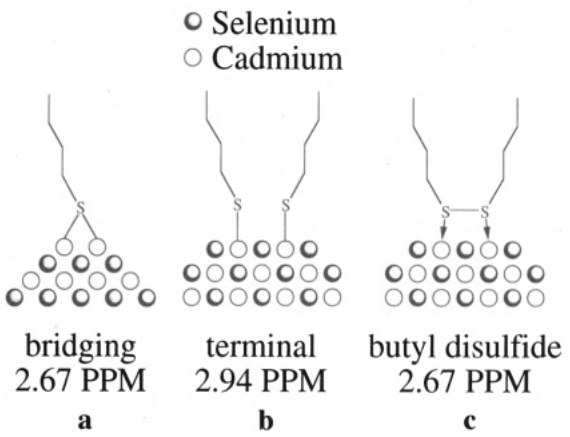

Figure 4. (a) Butanethiolate ligand bridging two surface cadmium ions. (b) Butanethiolate ligands can also form terminal bonds to single cadmium ions. Terminally bound ligands on neighboring cadmium sites can interact. (c) Attached butyl disulfide datively bound to the surface, and easily desorbed.

crystallite solutions and that even without light some disulfide is produced. We have taken strict precautions to check samples prior to ambient light exposure and exposure to oxygen is minimized, but we cannot rule out catalytic generation due to the presence of small amounts of oxygen.

We have done a series of experiments in order to quantify the catalytic reaction of BuSH to form BuSSBu. All of these experiments involved the same concentration of BuSH and CdSe nanocrystallites in pyridine. We took purified oxygen-free BuSH solutions in pyridine, exposed them to ambient light for 2 days, and found a trace amount of BuSSBu was detected by GC-MS. Solutions of BuSH and CdSe nanocrystallites in pyridine were exposed to light for the same amount of time, and after precipitation with benzene, the GC showed a 15-fold increase in the BuSSBu production. We also found an increase in the dark reaction production of BuSSBu in the presence of nanocrystallites, but it was small compared to the light reaction.

We have also taken carefully washed CdSe nanocrystallites containing no BuSSBu and only bound BuS^- groups and exposed them to light. GC-MS analysis indicates that trace amounts of BuSSBu are formed. In addition the mass spectrum fragmentation pattern of the supernatant suggests the presence of a $Cd(SC_4H_9)_2{\cdot}C_5H_5N$ complex.

Discussion

Three unexpected features were observed in this study: first the difference in surface coverage after washing with benzene, next the appearance of a transient NMR triplet at 2.94 ppm, and finally the generation of BuSSBu. These results suggest that the bonding of thiolate groups to the nanocrystallite surface is more complex than previously believed.

To explain our data, we *postulate* that there are actually three types of bonding between cadmium and sulfur atoms at the CdSe surface. When the BuS^- groups first attach to the surface, some find sites bridging between two cadmium ions, similar to that in refs 6 and 8, forming strong bonds (Figure 4a). The H_2 NMR resonance for this type of bonding occurs at 2.67 ppm. Other butanethiolates are attached with single covalent bonds to individual cadmium ions, forming less table, terminally bonded intermediates leading to an H_2 triplet centered at 2.94 ppm (Figure 4b). These groups can equilibrate by migration on the nanocrystallite surface until they are attached to neighboring cadmium ions. Such an equilibration has also been observed by Holm and co-workers in $[Cd_4(SPh)_{10}]^{2-}$ complexes.[15]

Unfortunately we were unable to determine the $^{13}C-^{113}Cd$ (or $^{13}C-^{111}Cd$) couplings in our nanocrystallite samples even with very long collection times. Dance and Saunders[7] observed these couplings in a $[Cd_{10}S_4(SPh)_{16}]^{4-}$ cluster, which were assigned to the terminal thiolates ($J = 9$ and 9 Hz) and bridging thiolates ($J = 16$ and 20 Hz). Our 811 atom systems are much larger than these clusters, leading to slow-to-medium ligand exchange.[7,8,12] These exchange rates cause broad ^{13}C signals and make the resolution of these couplings difficult as has previously been reported.[8] In addition, our systems have a very small mass ratio of surface ligands and hence a low ^{13}C concentration of the observable surface groups.

We postulate that the trace amounts of BuSSBu found for the washed samples after exposure to light arise from cleavage of these single covalent bonds. Two BuS^- groups attached to neighboring cadmium ions may interact through their sulfur lone pairs (Figure 4b) to form a S−S bond (101.65 kcal/mol[16]), while breaking the covalent S−Cd bonds (49.8 ± 5.0 kcal/mol[16]). The details of this mechanism, such as the catalytic role of O_2 in trace amounts and whether surface detachment occurs before or after BuSSBu formation, are unknown. Charge neutrality requires the addition of two holes to the two thiolate anions. If the reaction occurs before detachment, the resulting BuSSBu would then be weakly attached to the nanocrystallite and should easily detach and enter the solution upon washing (Figure 4c). Until it desorbed, the BuSSBu would block two cadmium surface sites. This is consistent with the detection of BuSSBu in the products by GC-MS but not as a contaminant in the starting material. The NMR measurements suggesting that BuSSBu molecules do not attach to the CdSe nanocrystallite surface indicate that the BuSSBu groups passivate the surface only during formation and that once desorbed, it is not energetically favorable to reattach.

An alternative mechanism for butyl disulfide formation requires exposure to light. Photoexcitation of nanocrystallites with visible light generates holes (h^+) which can oxidize the attached thiolate ligands.[10] The oxidation is followed by bond breakage of the Cd−S bond and thiolate radical recombination to give the disulfide product (Figure 4). The resulting BuSSBu would then be weakly attached to the nanocrystallites and should detach easily and enter the solution, either spontaneously or in the washing process. The GC-MS data suggest that a photochemical process is the dominant mechanism in the formation of butyl disulfide. No detectable disulfide is freshly prepared, multiply precipitated BuS^--capped nanocrystallite samples is observed. From NMR measurements, again we find that BuSSBu molecules do not attach to the CdSe nanocrystallite surface. BuSSBu is not generated directly from BuSH, since none is observed by NMR of solutions without nanocrystallites in the time frame of our measurements.

If we assume that all of the NMR resonance at 2.67 ppm for the washed sample corresponds to *bridge-bonded* butanethiolate,[8] with each ligand attached to a pair of cadmium ions, then 37.4% of the surface cadmium ions are passivated. From our data we cannot determine the exact degree of surface coverage before washing, but the nanocrystallite could be completely passivated. Elemental analysis data on the washed sample indicate enough pyridine to completely passivate the surface where the BuSSBu was removed. Before washing, the 2.67 ppm signal arises from contributions from bridged BuS^-, adsorbed BuSSBu, and free BuSSBu. If we assume that there is no free BuSSBu, we obtain a coverage of 133%, so there must be some free BuSSBu even before the nanocrystallite sample is washed for GC-MS analysis. This could be the reason for the difference in the time independence of the photolumi-

nescence and the 2.67 ppm NMR peak intensity (Figure 3a), although the difference between bound and free BuSSBu on the photoluminescence has not been established.

In comparing these results with those for CdSe single crystals, two points should be noted. First, nanocrystallites have far more defects than the commercially available single crystals used in refs 9 and 10. In addition, the nanocrystallite surfaces show no evidence of faceting, and their overall spherical shape suggests numerous steps along the surface. Such steps would provide more opportunities for thiolate ligands to bond in a bridging fashion, but the number of such sites is difficult to quantify.

While our results do not disprove the dead layer model, which describes how surface ligands alter the semiconductor photoluminescence, the penetration depth for the idealized single crystal is clearly not applicable here. We observe greater photoluminescence intensity from thiolate-capped than from pyridine-capped nanocrystallites, in qualitative agreement with this model. However, the reason for the agreement could arise either from the perturbation of the semiconductor band structure due to quantum confinement or from the presence of defects with high luminescence efficiency.

Our surface coverage results for BuS^--capped CdSe nanocrystallites are significantly higher than that for the phenylthiolate-capped CdS nanocrystallites, and several factors could be responsible.[5] It is clear that the steric requirements for phenyl thiolate versus butyl thiolate are more demanding, leading to significantly reduced coverage. The other possibility is that some bridge bonding may occur in phenyl thiolate-capped CdS nanocrystallites. A bridge bond fills two Cd sites, as opposed to a single site covered by a terminal bond. We have found consistency in coverage results for our samples studied by ^1H NMR and energy-dispersive spectroscopy, to within the experimental errors of these measurements. It is important to note, however, that we have found differences in the degree of coverage with the handling conditions of the CdSe nanocrystallites.

Conclusions

These results add new features to the current understanding of bonding at the CdSe nanocrystallite surface. We have shown that after careful preparation and purification of nanocrystallite samples, ^1H NMR can be used to distinguish free molecules in solution from attached ligands on a nanocrystallite surface. This NMR analysis can be used to quantify the average number of attached passivation groups per nanocrystallite. The NMR results have been used to study the kinetics of ligand attachment, which revealed more complex surface chemistry than previously believed. These results have been related to optical emission measurements which have been used extensively to characterize CdSe nanocrystallites and bulk CdSe surfaces.

Acknowledgments. S.A.M. would like to acknowledge support from the National Science Foundation through award DMR-925308 and the ACS Petroleum Research Fund through Grant ACS-PRF25025-G6. R.D.M. would like to acknowledge support from the National Science Foundation through award CHE-9201198 and the ACS Petroleum Research Fund through Grant ACS-PRF24953-G7P. In addition the help of J. Newbury was greatly appreciated.

References and Notes

(1) Steigerwald, M. L.; Alivisatos, A. P.; Gibson, J. M.; Harris, T. D.; Kortan, R.; Muller, A. J.; Thayer, A. M.; Douglass, D. C.; Brus, L. E. *J. Am. Chem. Soc.* **1988**, *110*, 3046. Bawendi, M. G.; Wilson, W. L.; Rothberg, L.; Carroll, P. J.; Jedju, T. M.; Steigerwald, M. L.; Brus, L. E. *Phys. Rev. Lett.* **1990**, *65*, 1623.

(2) Hilinski, E. F.; Lucas, P. A.; Wang, Y. *J. Chem. Phys.* **1988**, *89*, 3435.

(3) O'Neil, M.; Marohn, J.; McLendon, G. *J. Phys. Chem.* **1990**, *94*, 4356.

(4) Majetich, S. A.; Carter, A. C. *J. Chem. Phys.* **1993**, *97*, 8727.

(5) Sachleben, J. R.; Wooten, E. W.; Emsley, L.; Pines, A.; Colvin, V. L.; Alivisatos, A. P. *Chem. Phys. Lett.* **1992**, *198*, 43.

(6) Herron, N.; Calabrese, J. C.; Farneth, W. E.; Wang, Y. *Science* **1993**, *259*, 1426.

(7) Dance, I. G.; Saunders, J. K. *Inorg. Chim. Acta* **1985**, *96*, L71.

(8) Carson, G. K.; Dean, P. A. W.; Stillman, M. J. *Inorg. Chim. Acta* **1981**, *56*, 59.

(9) Lisensky, G. C.; Penn, R. L.; Murphy, C. J.; Ellis, A. B. *Science* **1990**, *248*, 840. Murphy, C. J.; Ellis, A. B. *Polyhedron* **1990**, *9*, 1913. Meyer, G. J.; Lisensky, G. C.; Ellis, A. B. *J. Am. Chem. Soc.* **1980**, *102*, 3671. Zhang, J. Z.; Geselbracht, M. J.; Ellis, A. B. *J. Am. Chem. Soc.* **1993**, *115*, 7789. Hollingsworth, R. E.; Sites, J. R. *J. Appl. Phys.* **1982**, *53*, 5357.

(10) Thackeray, J. W.; Natan, M. J.; Ng, P.; Wrighton, M. S. *J. Am. Chem. Soc.* **1986**, *108*, 3570. Hickman, J. J.; Wrighton, M. S. *J. Am. Chem. Soc.* **1991**, *113*, 4440. Bard, A. J.; Bocarsly, A. B.; Fan, F. F.; Walton, E. G.; Wrighton, M. S. *J. Am. Chem. Soc.* **1980**, *102*, 3671. Natan, M. J.; Thackeray, J. W.; Wrighton, M. S. *J. Phys. Chem.* **1986**, *90*, 4089.

(11) Steigerwald, M. L.; Alivisatos, A. P.; Gibson, J. M.; Harris, T. D.; Kortan, R.; Muller, A. J.; Thayer, A. M.; Duncan, T. M.; Douglas, D. C.; Brus, L. E. *J. Am. Chem. Soc.* **1988**, *110*, 3046.

(12) Saunders, J. K. M.; Hunter, B. K. *NMR Spectroscopy*; Oxford: New York, 1987; Chapter 3.

(13) Majetich, S.; Newbury, J.; Newbury, D. In *Determining Nanoscale Physical Properties of Materials by Microscopy and Spectroscopy*; Sarikaya, M., Ed.; MRS. Symp. Proc., *332*, 331 (1994).

(14) Lippens, P. E.; Lannoo, M. *Phys. Rev. B* **1989**, *39*, 10935.

(15) Hagen, K. S.; Stephan, D. W.; Holm, R. H. *Inorg. Chem.* **1982**, *21*, 3928.

(16) *CRC Handbook of Chemistry and Physics*, 73rd ed.; Little, D. R., Ed.; CRC Press: Boca Raton, FL, 1992–1993.

JP942105S